Initial state in relativistic heavy ion collisions

Author: Alba Ribera Paulí
Facultat de Física, Universitat de Barcelona, Diagonal 645, 08028 Barcelona, Spain.

Advisor: Volodymyr Magas
(Dated: January 15, 2019)

Abstract: At high temperatures or densities a state of matter formed by deconfined quarks and gluons emerges: the QGP. These conditions were present in the early universe and are replicable in the laboratory through relativistic heavy ion collisions. In peripheral collisions the system seems to be sensitive to vorticity due to the large initial angular momentum. This is thought to cause polarization, which is measurable through the spin of the emitted particles. Experimental data shows asymmetry between Λ and $\overline{\Lambda}$ polarization, whose origin is not yet clear.

In this paper we examine an initial state model to describe QGP evolution that applies Bjorken-like solution streak by streak in the collision transverse plane. The original model distributes energy and baryons along each streak, whereas our proposal homogeneously distributes baryons only at the extremes, while energy is kept as before. This extreme distribution has led to a new vorticity configuration that potentially could explain the observed differences between Λ and $\overline{\Lambda}$ polarization.

I. INTRODUCTION

Quark properties are challenging to study since they are confined within hadrons. Quantum chromodynamics (QCD) studies the strong interaction force between quarks, antiquarks and gluons that bind them together - collectively called partons. QCD predicts quark deconfinment ($\alpha_{QCD} \to 0$) at high temperatures or densities, enabling quasi-free partons to form a locally thermally equilibrated state of matter called quark gluon plasma (QGP) describable by an Equation of State (EoS) [1]. These extreme conditions are of high interest as they were present in the early universe, only few microseconds after the Big Bang [2]. At the present time they can be achieved in the laboratory through relativistic heavy ion collisions.

The RHIC at Brookhaven National Laboratory was the first heavy ion collider built, operating since 2000. At RHIC the beams are accelerated up to 100 GeV/nucl ($\sqrt{s_{NN}} = 200GeV$) in Au+Au reactions. A minuscule fireball of QGP is created, immediately cools down and thousands of pions and other elementary particles arise, central collisions being the most productive [2]. Before RHIC, QGP was expected to be a highly viscous and weakly coupled gaseous plasma. Instead, conclusions from experimental data led to the lowest viscosity fluid ever observed, almost a "perfect" liquid [3]. Currently CERN's LHC is the most energetic heavy ion collider, giving access to a deeper understanding of QGP like jet quenching phenomenon [4], not covered in this paper.

In the following sections we will develop an initial state model for further hydrodynamical evolution and study its development and outcome. In section II we will briefly review one of the simplest hydrodynamic models to describe QGP: the Bjorken model. In section III we will present our initial state model based on individual streak-streak collisions. We will study 2 different baryon density distributions: in section III one from [5] and in section IV another based on original Bjorken ideas and thought to be as much different from the first one as possible. In section V we will describe the resulting vorticities from these distributions. Finally, in section VI we will summarize and discuss the results. We will use natural units throughout the paper, with $c = 1$.

II. BJORKEN MODEL

Based on the mentioned perfect fluid behaviour, ideal relativistic hydrodynamics is appropriate to describe QGP. There are several analytical solvable models such as Landau, spherical fireball or Bjorken. The most suitable for ultra-relativistic energy is the Bjorken model [6].

The Bjorken model assumes colliding nuclei acting transparent to each other as they interpenetrate, so their valence quarks almost keep their rapidity, yet develop a chromo-electric field due to colour charge exchange [6]. The Bjorken model seems to be a good description for the initial period of the most energetic collisions.

The conservation laws for a perfect fluid are [6]:

$$\partial_\mu(N^\mu) = \partial_\mu(nu^\mu) = 0, \tag{1}$$

$$\partial_\mu(T^{\mu\nu}) = \partial_\mu[(e+P)u^\mu u^\nu - Pg^{\mu\nu}] = 0, \tag{2}$$

In order to solve these equations we require initial conditions and an EoS.

Milne space-time coordinates proper time τ and geometric rapidity η fit the problem better than Cartesian coordinates [6], whose respective transformations are:

$$z - z_0 = \tau sinh(\eta), \qquad t - t_0 = \tau cosh(\eta), \tag{3}$$

Following the Bjorken model, let us assume that all the physical quantities depend on τ but not on η, as it remains constant in the examined mid-rapidity region: $e = e(\tau)$, $p = p(\tau)$, $T = T(\tau)$ [6]. We obtain the following basic differential equations of Bjorken hydrodynamic model:

$$\frac{\partial n}{\partial \tau} = -\frac{n}{\tau}, \qquad \frac{\partial e}{\partial \tau} = -\frac{(e+P)}{\tau}, \tag{4}$$

where P is the pressure.

Using the relativistic ideal gas EoS: $P = e/3$ [1, 6]:

$$n(\tau) = n(\tau_0)\left(\frac{\tau_0}{\tau}\right), \qquad e(\tau) = e(\tau_0)\left(\frac{\tau_0}{\tau}\right)^{4/3}, \quad (5)$$

Eq. (5) describe the development of the partons during the QGP period up to rehadronization.

III. INITIAL STATE MODEL

In the following section we will briefly describe the initial state model for hydrodynamic simulation developed in [5], which should be consulted for further explanation. This model sets the starting point for our research on vorticity described in sections IV and V. It is worth mentioning that this model satisfies all conservation laws, including strong initial angular momentum, and can be applied to both Cartesian and Milne coordinate systems.

A. Independent streak-streak collisions

Consider a non-central Au+Au collision at energy per nucleon $\epsilon = 100 GeV/nucl$ and impact parameter $b = (r_{Au} + r_{Au})/2$. The collision region is structured as a 3 dimensional grid, in our case of $0.25 fm$ long cubic cells. Due to its relativistic energy, the projectile and the target are Lorentz contracted in the propagation axis and their momenta are Lorentz elongated. Taking this into consideration, the cell size in this axis has to be decreased: $\Delta z = 0.05 fm$ shows a good compromise simulation resources and timewise.

According to the Bjorken model, the transverse expansion can be disregarded during the initial post-collision time period. Consequently, the collision can be described as a collection of individual streak-streak collisions, each one assumed to follow Bjorken flow expansion on its own c.m. frame [5]. Independent streak-streak evolution is illustrated in Fig.(1).

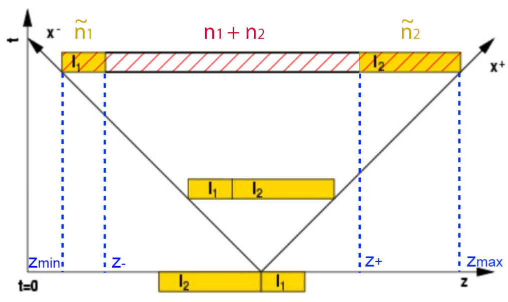

FIG. 1: Qualitative illustration of one streak-streak collision and subsequent evolution. Reprinted from [12] with blue and red elements as add-ons.

For each streak i the following pre-collision quantities are known: total baryon charge ($N_i = N_{1,i} + N_{2,i}$), total kinetic energy ($E_i = E_{1,i} + E_{2,i}$) and total momentum in the longitudinal direction ($P_{iz} = P_{2,iz} - P_{1,iz}$). All three should remain constant after the collision.

Let us define a $\tau = ct$ hypersurface normal four vector: $d^3\Sigma_\mu = \tau \Delta x \Delta y u_\mu d\eta$. Using the conservation laws we can calculate the conserved quantities crossing the hypersurface for each streak i at $\tau = \tau_0$ as follows:

$$\begin{aligned} dN_i &= d^3\Sigma_\mu N_i^\mu = n_i(\tau_0)\tau_0 A d\eta_i, \\ N_i &= n_i(\tau_0)\tau_0 A \Delta\eta_i, \end{aligned} \quad (6)$$

$$\begin{aligned} dE_i &= d^3\Sigma_\mu T_i^{0\mu} = e_i(\tau_0)\tau_0 A cosh(\eta_i) d\eta_i, \\ E_i &= 2e_i(\tau_0)\tau_0 A sinh(\Delta\eta_i/2) cosh(<\eta_i>), \end{aligned} \quad (7)$$

$$\begin{aligned} dP_{iz} &= d^3\Sigma_\mu T_i^{z\mu} = e_i(\tau_0)\tau_0 A sinh(\eta_i) d\eta_i, \\ P_{iz} &= 2e_i(\tau_0)\tau_0 A sinh(\Delta\eta_i/2) sinh(<\eta_i>), \end{aligned} \quad (8)$$

where $A = \Delta x \Delta y$, $\Delta\eta_i = (\eta_{max,i} - \eta_{min,i})$ and $<\eta_i> = (\eta_{max,i} + \eta_{min,i})/2 = Artanh(P_{iz}/E_i)$.

Therefore, by choosing appropriate values for τ_0 and $\Delta\eta_i$ this model gives homogeneous baryon and energy distributions in (τ, η) coordinates in the $[\eta_{min,i}, \eta_{max,i}]$ region. Using Eq.(3) and Eq.(5) we can know these initial state distributions in (t, z) coordinates.

B. Laboratory reference frame

In the previous subsection we have considered each streak on its c.m. frame. Once we want to study the whole collision at the laboratory frame we need to consider in addition each streak initial $[t_{0,i}, z_{0,i}]$ coordinates. To do so, we assume: $\tau_i(\eta_i = \langle\eta_i\rangle) = \tau_0$, $z_i(\tau_i = \tau_0) = 0$ and $e_i(\tau_i = \tau_0) = e_c$ [1] , which using Eq.(3) leads to:

$$z_{0i} = -\tau_0 sinh(\langle\eta_i\rangle), \quad (9)$$

$$t_{0i} = \sqrt{\tau_0^2 + z_{0i}^2}, \quad (10)$$

Based on literature, the 2 free parameters are set to $\Delta\eta = 2$ for the central streak and $\tau_0 = 1 fm$.

We also need to set a final global time T_{fin}. Its minimum value is defined as: $T_{fin} = max\{t_i, i = 1, ..., n\}$, which in our case has a value of $T_{fin} = 1.77 fm$ as shown in Fig.(2). This procedure ensures that all n streaks satisfy the conditions to be evaluated with hydrodynamic Bjorken equations.

At this point we are ready to calculate energy and baryon densities using Eq.(5). Baryon distribution for several streaks is illustrated in Fig.(4) a).

[1] This condition is different from the one used in [5]. For high impact parameters ($\geq 0.1 b_{max}$) the results are practically the same, but our version works well also for semi-central and central collisions.

Considering Eq.(1) and Eq.(2) we can calculate total baryon number and energy at some given t:

$$N_{total} = \sum_{x,y,z} n(t,x,y,z)\gamma(t,x,y,z)\Delta V, \tag{11}$$

$$E_{total} = \sum_{x,y,z} \frac{e(t,x,y,z)}{3}[4\gamma^2(t,x,y,z) - 1]\Delta V, \tag{12}$$

where $\Delta V = A\Delta z$ is the cell volume.

IV. EXTREME BARYON DENSITY DISTRIBUTION

Peripheral heavy ion collisions have a large initial angular momentum that is responsible for the shear flow in the fluid dynamics, as illustrated in Fig.(3), which arises a vorticity stronger than the one produced by random fluctuations [7].

Recent studies suggest that this vorticity induces polarization to the resulting hadrons, as explained in [3, 7–9]. Polarization has been experimentally observed for Λ and $\overline{\Lambda}$ hyperons [3], which show an asymmetry. Whereas Λ polarization has been explained in [7, 8], $\overline{\Lambda}$ has not yet been explained. In [9] it was suggested the explanation could be related to energy flow and baryon flow being different from each other. The main purpose of this paper is to design a set of initial conditions different from the one already evaluated in [7] and in section III B that lead to great difference between baryon and energy flows.

Based on discussion in [9], our suggestion is to modify the baryon density distribution. In the previous section partons occupied the streak of length $[z_{min,i}, z_{max,i}]$. Instead, we now force them to be in two separated regions of $\ell_i^1(t_{0,i})$ and $\ell_i^2(t_{0,i})$ lengths based on the original Bjorken idea, placed at the extremes as illustrated in Fig.(1). This arrangement keeps the projectile and target partons unmixed in $[z_{min,i}, z_{-,i}]$ and $[z_{+,i}, z_{max,i}]$ regions. Energy, on the other hand, occupies the $[z_{min,i}, z_{max,i}]$ region due to the creation of the chromo-electric field as a result of quark colour exchange like in the previous scenario.

Let us define a $t = T_{fin} = ct$ hypersurface normal four vector: $d^3\Sigma_\mu = \Delta x\Delta y u_\mu \gamma(z)dz$. Analogously to Eq.(6), we can count the baryons crossing the hypersurface as:

$$dN_i = d^3\Sigma_\mu N_i^\mu = d^3\Sigma_\mu \widetilde{n}_i u_i^\mu = A\widetilde{n}_i\gamma_i(z_i)dz_i, \tag{13}$$

$$N_i = A\widetilde{n}_i \int \gamma_i(z_i)dz_i = A\widetilde{n}_i T_{fin}\left[arcsin\left(\frac{z_i}{T_{fin}}\right)\right], \tag{14}$$

At this point the only unknown quantity is the extreme baryon density $\widetilde{n_i}^{1/2}$, since $N_i^{1/2}$ is known and conserved from the pre-collision value $N_i^{1/2} = \gamma_0\rho_0 A\ell_i^{1/2}$, which leads to:

$$\widetilde{n}_i^1 = \frac{\gamma_0\rho_0}{T_{fin}}\left[\frac{\ell_i^1}{\arcsin\left(\frac{z_{-,i}}{T_{fin}}\right) - \arcsin\left(\frac{z_{min,i}}{T_{fin}}\right)}\right],$$

$$\widetilde{n}_i^2 = \frac{\gamma_0\rho_0}{T_{fin}}\left[\frac{\ell_i^2}{\arcsin\left(\frac{z_{max,i}}{T_{fin}}\right) - \arcsin\left(\frac{z_{+,i}}{T_{fin}}\right)}\right], \tag{15}$$

The results for homogeneous n and extreme $\widetilde{n}$ baryon distributions can be compared in Fig.(4), which show strong variation: mixed partons in $[z_{min,i}, z_{max,i}]$ versus unmixed partons in $[z_{min,i}, z_{-,i}]$ and $[z_{+,i}, z_{max,i}]$ regions. We expect to achieve such differences in vorticity results as well. In both cases the asymmetry produced in peripheral streaks is clearly shown.

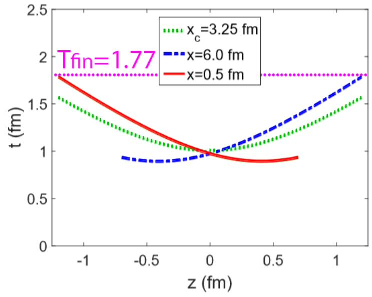

FIG. 2: Initial [t,z] configuration for central and extreme streaks. $T_{fin} = max\{t_i\} = 1.77fm$. Reprinted from [5] with magenta elements as add-ons.

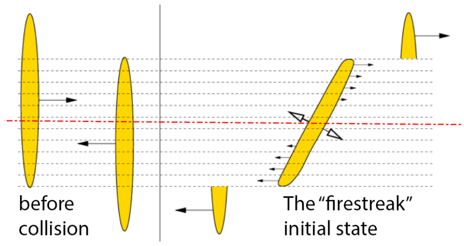

FIG. 3: Illustrative representation of shear in a peripheral heavy ion collision. Reprinted from [12].

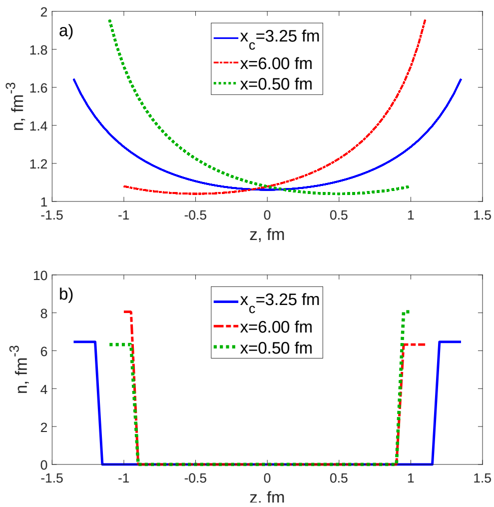

FIG. 4: Homogeneous baryon distribution as in [5] (a) and extreme baryon distribution (b) at time $t = T_{fin} = 1.77fm$ for 3 streaks of different x location: central streak at $x = 3.25fm$ and 2 peripheral streaks at $x = 0.50fm$ and $x = 6.00fm$. The parameters of this simulation are: $\epsilon = 100GeV/nucl$, $b = (r_{Au} + r_{Au})/2$, $\tau_0 = 1fm$, $\Delta\eta_c = 2$.

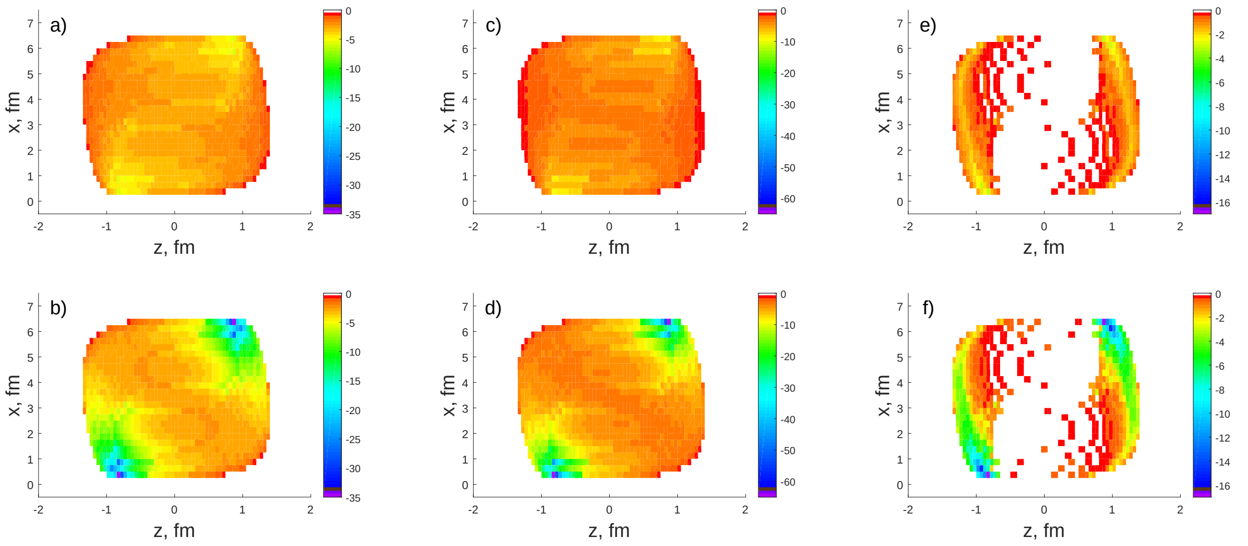

FIG. 5: Energy density weighted total vorticity for classical (a) and relativistic (b) scenarios. Homogeneous baryon density weighted total vorticity for classical (c) and relativistic (d) scenarios. Extreme baryon density weighted total vorticity for classical (e) and relativistic (f) scenarios. This simulations has the same parameters as Fig.(4).

For n distribution, N post-collision value shows a 3% error compared to pre-collision value, whereas E arises a larger discrepancy. The cause of this discrepancy are the boarders that are imposed in our simulation, determined by $\Delta\eta$. Vacuum being outside, boarders undergo a strong pressure gradient. To avoid matter expansion some work is done on the boarder surface, thus energy conservation can be expressed as: $E(\tau_0) = E(\tau) + W(\tau)$. For deeper development on energy conservation consult [10].

For $\widetilde{n}$ distribution the discrepancy is larger. Due to baryon extreme distribution imposition, we are required to adjust Δz to achieve a similar precision than the one before. A value of $\Delta z = 0.01fm$ lowers the discrepancy to a 10%. To improve efficiency we have defined a rescale value for each streak as well.

V. VORTICITY

In the reaction plane [x,z] classical and relativistic vorticities are respectively defined as [7]:

$$\omega_y^{clas} = \frac{1}{2}(\partial_z v_x - \partial_x v_z), \tag{16}$$

$$\omega_y^{rel} = \frac{1}{2}(\partial_z \gamma v_x - \partial_x \gamma v_z), \tag{17}$$

Since Bjorken model disregards transverse expansion, we can consider $v_x = v_y = 0$.

We follow the PIC method to estimate the vorticity as described in [11] both for classical and relativistic scenarios, which accounts for the nearest four side and four corner neighbouring cells:

$$\omega_y^{clas} = -\frac{1}{2}\left[\frac{(v_z^{+0} - v_z^{00}) + (v_z^{00} - v_z^{-0})}{2\Delta x} + \right. \\ + \frac{(v_z^{++} - v_z^{0+}) + (v_z^{0-} - v_z^{--})}{4\Delta x} + \\ \left. + \frac{(v_z^{+-} - v_z^{0-}) + (v_z^{0+} - v_z^{-+})}{4\Delta x}\right], \tag{18}$$

$$\omega_y^{rel} = \gamma^{00}\omega_y^{clas} - \frac{v_z^{00}}{8}\left[\frac{(\gamma^{+0} - \gamma^{00}) + (\gamma^{00} - \gamma^{-0})}{2\Delta x} + \right. \\ + \frac{(\gamma^{++} - \gamma^{00}) + (\gamma^{00} - \gamma^{--})}{4\Delta x} + \\ \left. + \frac{(\gamma^{+-} - \gamma^{00}) + (\gamma^{00} - \gamma^{-+})}{4\Delta x}\right], \tag{19}$$

where +,- and 0 indicate each neighbouring cell's [x,z] location relative to the current cell.

In order to achieve a more accurate approximation to vorticity development, we will define several weights ρ that will depend on either energy or baryon densities.

Let us define two weights ρ^n and $\rho^{\widetilde{n}}$ depending on parton quantity within the cell in relation to average cell parton quantity for n and $\widetilde{n}$ distributions respectively:

$$\rho_{ik}^n = \frac{N_{ik}}{N_{tot}/N^{\underline{o}}_{cell}}, \qquad \rho_{ik}^{\widetilde{n}} = \frac{\widetilde{N}_{ik}}{\widetilde{N}_{tot}/N^{\underline{o}}_{cell}}, \tag{20}$$
$$N_{ik} = n_{ik}\gamma_{ik}\Delta V, \qquad \widetilde{N}_{ik} = \widetilde{n}_{ik}\gamma_{ik}\Delta V,$$

Similarly, energy weight ρ^e is defined as the quotient of the cell's energy divided by the average cell energy:

$$\rho^e_{ik} = \frac{E_{ik}}{E_{tot}/N^{\underline{o}}_{cell}}, \qquad (21)$$
$$E_{ik} = T^{00}_{ik} = \frac{e_{ik}}{3}(4\gamma^2_{ik} - 1)\Delta V,$$

For illustrative purpose, we will use the vorticity sum up in all layers, defined as:

$$\Omega^{(e/n/\tilde{n})}_{i_x,k_z} = \sum_{j_y} \rho^{(e/n/\tilde{n})}(i_x, k_z, j_y)\omega_y(i_x, k_z, j_y), \qquad (22)$$

Results for each 3 weighted total vorticities can be compared in Fig.(5). Total vorticities in cases a), b), c) and d) are rather similar, as expected. However, total vorticity of our new extreme baryon distribution is clearly different, so it could be interesting to study its resulting polarization and compare it to experimental data.

VI. CONCLUSIONS AND DISCUSSION

In this paper we have introduced the phenomenon of a state of matter that behaves almost like a perfect fluid and emerges under high temperatures or densities: the QGP. These conditions were present in the early universe and can be achieved through relativistic heavy ion collisions at the laboratory. We have pointed out the convenience of using Bjorken hydrodynamic model and presented a Bjorken solution-based initial state model developed in [5] that describes QGP evolution by treating the collision as a set of individual streak-streak collisions.

We have considered a peripheral Au+Au collision at $\epsilon = 100GeV/nucl$ and $b = (r_{Au} + r_{Ar})/2$. We have studied its classical and relativistic vorticity development in the reaction plane and presented total classical and relativistic vorticities weighted according to e in Fig.(5) a) and b) and according to n in Fig.(5) c) and d). Results show vorticity is relevant due to its vast magnitude, therefore should not be ignored as it used to be in early QGP models.

Evidence of this huge vorticity has lead scientists to develop a recent theory: the spins of the resulting particles tend to align to the vorticity, and consequently to the angular momentum of the system [3]. Polarity of the emitted hadrons has been experimentally measured by the STAR detector at RHIC, which is a difficult task for most of the created particles except for Λ and $\overline{\Lambda}$ hyperons. QGP is likely to be the hottest and least viscous fluid ever observed in the laboratory, and STAR observations add another characteristic: the most vortical fluid ever produced in the laboratory.

The observed and unexplained differences between Λ and $\overline{\Lambda}$ polarizations motivated us to develop a new model of initial state. Based on [9], we have modified the Bjorken-based initial state model in [5]. The purpose was to set certain initial conditions that would cause difference between energy and baryon flows. Our suggestion has consisted in adjusting the baryon density distribution after the collision of two streaks: whereas the original model distributed the mixed partons along the $[z_{min}, z_{max}]$ region, ours place them homogeneously only at 2 unmixed $[z_{min}, z_-]$ and $[z_+, z_{max}]$ regions at the extremes. Vorticity development for this configuration has shown significant differences from previous scenario, as shown in Fig.(5) e) and f). Taking these results into consideration, it would be interesting to continue this research path by relating this vorticity to polarization and compare theoretical development to experimental data.

Acknowledgments

First of all I would like to thank my advisor V. Magas for all his knowledge and indispensable support in the fulfilment of this paper. I would also like to thank my family for encouraging me in all my challenges.

[1] R. Snellings [ALICE collaboration], Fundamental Interactions (2007) pp. 142-169.
[2] T. Ludlam and L. McLerran, Phys. Today **56N10** (2003) 48. doi:10.1063/1.1629004.
[3] L. Adamczyk *et al.* [STAR Collaboration], Nature **548** (2017) 62 doi:10.1038/nature23004 [arXiv:1701.06657 [nucl-ex]].
[4] A. Angerami, (2012), arXiv:1208.5043 [nucl-ex].
[5] V. K. Magas, J. Gordillo, D. Strottman, Y. L. Xie and L. P. Csernai, Phys. Rev. C **97** (2018) no.6, 064903 doi:10.1103/PhysRevC.97.064903 [arXiv:1712.00283 [nucl-th]].
[6] L. P. Csernai, *Introduction to relativistic heavy ion collisions*, Chichester, UK: Wiley (1994) 310 p.
[7] L. P. Csernai, V. K. Magas and D. J. Wang, Phys. Rev. C **87** (2013) no.3, 034906 doi:10.1103/PhysRevC.87.034906 [arXiv:1302.5310 [nucl-th]].
[8] F. Becattini, I. Karpenko, M. Lisa, I. Upsal and S. Voloshin, Phys. Rev. C **95** (2017) no.5, 054902 doi:10.1103/PhysRevC.95.054902 [arXiv:1610.02506 [nucl-th]].
[9] L. P. Csernai, J. I. Kapusta and T. Welle, arXiv:1807.11521 [nucl-th].
[10] V. K. Magas and L. P. Csernai, Phys. Lett. B **663** (2008) 191 doi:10.1016/j.physletb.2008.04.036 [arXiv:0804.3520 [nucl-th]].
[11] PhD Thesis, Dujuan Wang, *Rotation and Turbulence in Peripheral Heavy Ion Collisions*, University of Bargen, Norway (2014).
[12] V. K. Magas, L. P. Csernai and D. Strottman, PRC 64 (2001) 014901, NPA 712 (2002) 167.